Accepted Manuscript

Predictions of critical transitions with non-stationary reduced order models

Christian L.E. Franzke

PII: S0167-2789(13)00221-2
DOI: http://dx.doi.org/10.1016/j.physd.2013.07.013
Reference: PHYSD 31414

To appear in: *Physica D*

Received date: 15 January 2013
Revised date: 13 July 2013
Accepted date: 18 July 2013

Test of tipping point predictions with reduced order stochastic models

Ensemble approach for tipping point prediction

Ensemble approach is robust in predicting tipping points

Predictions of Critical Transitions with Non-Stationary Reduced Order Models

Christian L. E. Franzke

British Antarctic Survey, Natural Environment Research Council, Cambridge, UK

Phone: +44 (0) 1223221350
Fax: +44 (0) 1223221226
E-mail: christian.franzke@gmail.com

Abstract

Here we demonstrate the ability of stochastic reduced order models to predict the statistics of non-stationary systems undergoing critical transitions. First, we show that the reduced order models are able to accurately predict the autocorrelation function and probability density functions (PDF) of higher dimensional systems with time-dependent slow forcing of either the resolved or unresolved modes. Second, we demonstrate that whether the system tips early or repeatedly jumps between the two equilibrium points (flickering) depends on the strength of the coupling between the resolved and unresolved modes and the time scale separation. Both kinds of behaviour have been found to preceed critical transitions in earlier studies. Furthermore, we demonstrate that the reduced order models are also able to predict the timing of critical transitions. The skill of various proposed tipping indicators are discussed.

Keywords: Stochastic Modeling, Tipping Points, Model Reduction, Non-Stationarity, Bifurcation, Critical Transition

1. Introduction

Many complex dynamical systems exhibit so-called critical transition or tipping points in which the system approaches a bifurcation point which can lead to sudden and possibly irreversible changes. Even small changes in the control parameter or forcing can lead to a large jump to a different state with possibly catastrophic outcomes. Examples of such tipping points in the real world range from epileptic seizures (McSharry et al., 2003), financial market failures (Sornette and Johansen, 1997), ecosystems (Scheffer et al., 2001), fisheries (Biggs et al., 2009), abrupt shifts in ocean circulation (Monahan et al., 2008), paleoclimatic abrupt changes (Dakos et al., 2008; Lenton et al., 2008; Livina et al., 2011, 2013; Cimatoribus et al., 2013), irreversible decline of the Greenland Ice Sheet (Ridley et al., 2010) and loss of Arctic sea ice extent (Eisenmann and Wettlaufer, 2008; Wadhams, 2012). As these tipping points directly affect human well being and the economy it is of utmost importance to be able to forecast these sudden shifts in order to either avert them or at least mitigate their effects. Thus, the detection of early warning signals of imminent tipping points has attracted a lot of attention (Scheffer et al., 2009; Biggs et al., 2009; Dakos et al., 2008; Ditlevsen and Johnsen, 2010; Held and Kleinen, 2004; Kuehn, 2011, 2013; Lenton et al., 2008; Sieber and Thompson, 2012; Livina and Lenton, 2007; Livina et al., 2010, 2011, 2012).

Most tipping point detection methods are based on the theory of critical transitions and critical slowing down. Typical signs of an imminent tipping point are that the intrinsic transient response to perturbations slows down (Wissel, 1984; Held and Kleinen, 2004; Veraart et al., 2012), an increase in autocorrelation (Scheffer et al., 2009), an increase in variance (Ditlevsen and Johnsen, 2010) or in skewness (Guttal and Jayaprakash, 2008).

The slowing down is usually detected by computing the lag-1 autocorrelation value by using a sliding data window (Held and Kleinen, 2004) or by a so-called DFA propagator (Livina and Lenton, 2007). Evidence for an imminent tipping point is found when one of the indicators shows an increasing trend. Unfortunately this approach is sensitive to the used window length and the detrending procedure before the indicators are computed. Furthermore, the underlying assumption of the detrending procedure is that the time series over the window length can be considered to be stationary, which is contradictory to the original assumption that the system is approaching a bifurcation (Boettinger and Hastings, 2012b). Furthermore, there is also no real threshold value which needs to be crossed in order to signal that the system approaches the tipping point. Boettinger and Hastings (2012a) argue that most previous studies might be biased because they focus only on periods with a critical transition. They suggest that model based approaches, especially ensemble predictions, are less subject to this bias.

The above proposed tipping point indicators are all based on the analysis of observed time series. Since in most cases tipping points are singular events the ensemble approach is not feasible with just observational data; though Cimatoribus et al. (2013) used the Dansgaard-Oeschger events encoded in Greenland ice cores in an ensemble sense. However, in many situations tipping points are singular events which might not have happened or been observed before. An alternative approach is to use low-order dynamical models fitted to the observed data to predict tipping points (Carpenter and Brock, 2011). Here we will evaluate the possible use of reduced order stochastic models in predicting tipping points using an ensemble approach.

In a series of papers Majda et al. (1999, 2001, 2002, 2005, 2008, 2009) developed a systematic framework for the derivation of physics constrained reduced order models which are nonlinear and have state-dependent noise. Their ability to reproduce the statistics of high dimensional models of such quantities as probability density and autocorrelation functions has been shown by Franzke et al. (2005) and Franzke and Majda (2006). These systematic reduced order models are also skillful in reproducing the extreme value statistics and the predictability of extreme events of higher dimensional systems (Franzke, 2012).

The idea behind tipping point prediction is that the underlying essential dynamics can be represented by a potential well driven by additive white noise (Scheffer et al., 2009; Livina et al., 2013). This is based on bifurcation theory of low-dimensional Ordinary Differential Equations. However, in practical situations one has often an one-dimensional indicator time series (e.g. data from an ice core, measurement of the Meridional Overturning Circulation in the ocean) of a complex high-dimensional system. Using such a time series for tipping point prediction implicitly assumes either a weak coupling or time scale separation between the indicator time series and the remaining variables of the system. In this approach there is also a hidden assumption of an additive coupling between the observed indicator time series and the rest of the system. These approaches do not consider the possibility of multiplicative coupling which could lead to a state-dependent noise. For instance, this state-dependent noise could create a double well potential on its own with the deterministic dynamics playing no role in the creation of the double well potential (Sura et al., 2005) (see their figure 1). In such a system all transitions are purely noise driven. This illustrates the danger on relying upon purely data driven approaches since they are unlikely to be able to distinguish the dynamical causes of the potential well. The here proposed approach of using dynamical models also provides insight into the underlying dynamics and thus gives more confidence in the predictions.

In this study we will derive dynamical reduced order models which are driven by a slow forcing towards a bifurcation point. After demonstrating that the reduced order model reproduce the same tipping point behaviour we will elucidate the roles of time scale separation and coupling strength between resolved and unresolved modes and how they affect the tipping behaviour: whether the systems undergoes a clean tipping or flickers between the two equilibrium states. Flickering has recently also been proposed as an indicator of an imminent tipping event (Veraart et al., 2012). Both kinds of behaviour have been found to preceed critical transitions. So far no explanation has been given on which properties of the underlying dynamics they depend. To elucidate the conditions under which one can expect a clean tipping or flickering is a major motivation of this study.

We will introduce the stochastic conceptual model which represents a minimal prototype climate model in Section 2. We discuss its performance when driven by time-dependent forcing in Section 3 and its ability to robustly predict tipping points in Section 4. In Section 4 we also discuss the robustness of the typically used tipping point prediction methods. We provide a summary of our results in section 5.

2. Stochastic Conceptual Model

In this section we describe the conceptual model which we are using in our study of tipping points. A similar version of this conceptual model has been used in previous studies (Majda et al., 2005, 2008; Franzke et al., 2007; Franzke, 2012). The conceptual model is 4 dimensional and contains the essential dynamics of more complex climate models even though it is of much lower dimensionality.

The conceptual model we are using in this study has two slow or climate variables denoted by (x_1, x_2). These two modes evolve slowlier than the other two modes (y_1, y_2). These two fast modes represent turbulent eddies and convective systems in the climate system which are in many climate models not fully resolved. In realistic systems there would be innumerable many fast modes, and in order to mimic their combined effect on the two slow climate modes we include damping and stochastic forcing $-\frac{\gamma}{\varepsilon}y + \frac{\sigma}{\sqrt{\varepsilon}}dW$ in the equations for y where W denotes a Wiener process. This approximation is motivated by the fact that these fast modes are associated with turbulent energy transfers and strong mixing. In this study we do not require a detailed description of these processes because we are only interested in their combined effect on the slow resolved modes and not in their detailed evolution. The stochastic climate model is given by

$$\begin{aligned}
dx_1 &= ((-x_2(L_{12}+a_1x_1+a_2x_2)+d_1x_1+F_1(t)) && \text{(1a)}\\
&\quad +\theta(L_{13}y_1+b_{123}x_2y_1+(c_{131}+c_{113})x_1y_1))\,dt && \text{(1b)}\\
dx_2 &= ((+x_1(L_{21}+a_1x_1+a_2x_2)+d_2x_2+F_2(t)) && \text{(1c)}\\
&\quad +\theta(L_{24}y_2+b_{213}x_1y_1+(e_{242}+e_{224})x_2y_2))\,dt && \text{(1d)}\\
dy_1 &= \left(-L_{13}x_1+b_{312}x_1x_2+c_{311}x_1x_1+F_3(t)-\frac{\gamma_1}{\varepsilon}y_1\right)dt+\frac{\sigma_1}{\sqrt{\varepsilon}}dW_1 && \text{(1e)}\\
dy_2 &= \left(-L_{24}x_2+e_{422}x_2x_2+F_4(t)-\frac{\gamma_2}{\varepsilon}y_2\right)dt+\frac{\sigma_2}{\sqrt{\varepsilon}}dW_2 && \text{(1f)}
\end{aligned}$$

The parameter ε controls the time-scale separation between the slow and fast variables. Energy conservation of the nonlinear operator requires that $b_{123}+b_{213}+b_{312}=0$, $c_{131}+c_{113}+c_{311}=0$ and $e_{242}+e_{224}+e_{422}=0$. The linear operator matrix $\mathbf{L}$ is skew-symmetric. The climate and fast modes are both linearly and nonlinearly coupled through triad and dyad interactions. Note that the forcing $\mathbf{F}(t)$ is time-dependent in contrast to earlier studies (Majda et al., 2005, 2008; Franzke et al., 2007; Franzke, 2012). We added a parameter θ in (1) with which we are able to control the strength of the interaction between the deterministic nonlinear dynamics and the fast unresolved modes.

To highlight the structural form of our conceptual model (1) we rewrite it as

$$d\mathbf{z} = (\mathbf{F}(t)+L\mathbf{z}(t)+B(\mathbf{z}(t),\mathbf{z}(t)))\,dt+\sigma d\mathbf{W}. \tag{2}$$

This is the same structural form as climate models have with a forcing $\mathbf{F}$, a linear operator L, a quadratic nonlinear operator B and additive noise forcing $d\mathbf{W}$. While most current climate models are deterministic there are a few numerical weather prediction models which have stochastic terms.

2.1. Explicit Stochastic Mode Reduction

We now apply the systematic stochastic mode reduction procedure (Majda et al., 1999, 2001, 2002) to the model (1) to obtain explicit reduced stochastic equations for the slow variables $\mathbf{x}$. The simplicity of the above model allows us to do the stochastic mode reduction directly using the equations without transforming it to the corresponding Fokker-Planck equation.

The stochastic differential equation (SDE) for the variable $\mathbf{y}$ in (1) is linear in $\mathbf{y}$. Thus, given $\mathbf{x}(t)$ its solution is

$$\begin{aligned} y_1(t) &= e^{-\frac{\gamma_1 t}{\varepsilon}} y_1(0) + \int_0^t e^{-\frac{\gamma_1(t-s)}{\varepsilon}} \left[-L_{13}x_1(s) + b_{312}x_1(s)x_2(s)\right. \\ &\quad \left. + c_{311}x_1(s)x_1(s) + F_3(s)\right] ds + g_1(t) \end{aligned} \tag{3}$$

where

$$g_1(t) = \frac{\sigma_1}{\sqrt{\varepsilon}} \int_0^t e^{-\frac{\gamma_1(t-s)}{\varepsilon}} dW_1(s) \tag{4}$$

and

$$\begin{aligned} y_2(t) &= e^{-\frac{\gamma_2 t}{\varepsilon}} y_2(0) + \int_0^t e^{-\frac{\gamma_2(t-s)}{\varepsilon}} \left[-L_{24}x_2(s) + e_{422}x_2(s)x_2(s)\right. \\ &\quad \left. + F_4(s)\right] ds + g_2(t) \end{aligned} \tag{5}$$

where

$$g_2(t) = \frac{\sigma_2}{\sqrt{\varepsilon}} \int_0^t e^{-\frac{\gamma_2(t-s)}{\varepsilon}} dW_2(s) \tag{6}$$

Inserting (3) and (5) into the first two equations in (1) for the variable $\mathbf{x}$ yields an exact, non-Markovian system of equations for $\mathbf{x}(t)$.

Since we are interested in the long time statistical behaviour of the climate variables $\mathbf{x}(t)$ as $\varepsilon \to 0$, we consider the asymptotic limit as $\varepsilon \to 0$ of the three terms on the right of (3) and (5). First we immediately have

$$e^{-\frac{\gamma_1 t}{\varepsilon}} y_1(0) \to 0 \tag{7}$$

$$e^{-\frac{\gamma_2 t}{\varepsilon}} y_2(0) \to 0 \tag{8}$$

Second, using integration by parts we find

$$\begin{aligned} &\int_0^t e^{-\frac{\gamma_1(t-s)}{\varepsilon}} \left[-L_{13}x_1(s) + b_{312}x_1(s)x_2(s) + c_{311}x_1(s)x_1(s) + F_3(s)\right] ds \\ &\qquad \to \frac{\varepsilon}{\gamma_1} \left[-L_{13}x_1(t) + b_{312}x_1(t)x_2(t) + c_{311}x_1(t)x_1(t) + F_3(t)\right] \end{aligned} \tag{9}$$

$$\begin{aligned} &\int_0^t e^{-\frac{\gamma_2(t-s)}{\varepsilon}} \left[-L_{24}x_2(s) + e_{422}x_2(s)x_2(s) + F_4(s)\right] ds \\ &\qquad \to \frac{\varepsilon}{\gamma_2} \left[-L_{24}x_2(t) + e_{422}x_2(t)x_2(t) + F_4(t)\right] \end{aligned} \tag{10}$$

Finally, it can be shown that $g_1(t)$ and $g_2(t)$ are itself approximatively white noise as $\varepsilon \to 0$ (Majda et al., 2001)

$$g_1(t)dt \to \sqrt{\varepsilon}\frac{\sigma_1}{\gamma_1}dW_1(t) \tag{11}$$

$$g_2(t)dt \to \sqrt{\varepsilon}\frac{\sigma_2}{\gamma_2}dW_2(t) \tag{12}$$

for this we use the fact that $g_1(t)$ and $g_2(t)$ are Gaussian and the two properties for any test function η

$$\mathbb{E}\left(\frac{1}{\varepsilon}\int_0^\infty \eta(t)g_j(t)dt\right) = 0 \tag{13}$$

and

$$\mathbb{E}\left(\frac{1}{\varepsilon}\int_0^\infty \eta(t)g_i(t)dt\right)\left(\frac{1}{\varepsilon}\int_0^\infty \eta(t)g_j(t)dt\right) \to \varepsilon\frac{\sigma_j^2}{\gamma_j^2}\delta_{ij}\int_0^\infty \eta^2(t)dt \tag{14}$$

We note, however, that, as an approximation of a process with finite correlation time, $dW_i(t)$ has to be interpreted in the Stratonovich sense (Gardiner, 1985).

Combining these formulas in the first two equations of (1), we obtain the following SDE transformed to Itô form with the noise induced drift (Gardiner, 1985):

$$
\begin{aligned}
dx_1(t) \;=\; & \left(-x_2(t)\left(L_{12}+a_1x_1(t)+a_2x_2(t)\right)+d_1x_1(t)+F_1(t)\right)dt \\
& +\theta\left(\frac{\varepsilon}{\gamma_1}\left(L_{13}F_3(t)-L_{13}L_{13}x_1(t)+b_{123}F_3(t)x_2(t)\right.\right. \\
& +L_{13}b_{312}x_1(t)x_2(t)-L_{13}b_{123}x_1(t)x_2(t)+L_{13}c_{311}x_1^2(t) \\
& +b_{312}b_{123}x_1(t)x_2^2(t)+b_{123}c_{311}x_2(t)x_1^2(t)+\left(c_{131}+c_{113}\right) \\
& \left.\left(c_{311}x_1^3(t)-L_{13}x_1^2(t)+b_{312}x_1^2(t)x_2(t)+F_3(t)x_1(t)\right)\right)dt \\
& +\varepsilon\frac{1}{2}\frac{\sigma_1^2}{\gamma_1^2}\left(b_{213}b_{123}x_1(t)+\left(L_{13}+b_{123}x_2(t)\right.\right. \\
& \left.\left.+\left(c_{131}+c_{113}\right)x_1(t)\right)\left(c_{131}+c_{113}\right)\right)dt \\
& \left.\sqrt{\varepsilon}\frac{\sigma_1}{\gamma_1}\left(L_{13}+b_{123}x_2(t)+\left(c_{131}+c_{113}\right)x_1(t)\right)dW_1(t)\right)
\end{aligned}
\tag{15a}
$$

$$
\begin{aligned}
dx_2(t) \;=\; & \left(x_1(t)\left(L_{21}+a_1x_1(t)+a_2x_2(t)\right)+d_2x_2(t)+F_2(t)\right)dt \\
& +\theta\left(\frac{\varepsilon}{\gamma_2}\left(L_{24}F_4(t)-L_{24}L_{24}x_2(t)+L_{24}e_{422}x_2^2(t)\right.\right. \\
& \left.+\left(e_{242}+e_{224}\right)\left(e_{422}x_2^3(t)-L_{24}x_2^2(t)+F_4(t)x_2(t)\right)\right)dt \\
& +\frac{\varepsilon}{\gamma_1}\left(-b_{213}L_{13}x_1(t)x_1(t)+b_{213}c_{311}x_1^3(t)\right. \\
& \left.+b_{213}b_{312}x_1(t)x_1(t)x_2(t)+b_{213}F_3(t)x_1(t)\right)dt \\
& +\varepsilon\frac{1}{2}\frac{\sigma_1^2}{\gamma_1^2}\left(b_{213}b_{123}x_2(t)+L_{13}b_{213}+\left(c_{131}+c_{113}\right)b_{213}x_1(t)\right)dt \\
& +\varepsilon\frac{1}{2}\frac{\sigma_2^2}{\gamma_2^2}\left(L_{24}+\left(e_{242}+e_{224}\right)x_2(t)\right)\left(e_{242}+e_{224}\right)dt \\
& +\sqrt{\varepsilon}\frac{\sigma_1}{\gamma_1}b_{213}x_1(t)dW_1(t) \\
& \left.+\sqrt{\varepsilon}\frac{\sigma_2}{\gamma_2}\left(L_{24}+\left(e_{242}+e_{224}\right)x_2(t)\right)dW_2(t)\right)
\end{aligned}
\tag{15b}
$$

Note that coarse graining time as $t \to \frac{t}{\varepsilon}$ amounts to setting $\varepsilon = 1$ (Majda et al., 1999, 2001; Franzke et al., 2005; Franzke and Majda, 2006).

To highlight the structural differences we rewrite the reduced model in the following form

$$
\frac{d\mathbf{x}}{dt} = \tilde{\mathbf{F}}(t)+\tilde{L}\mathbf{x}(t)+\tilde{B}(\mathbf{x}(t),\mathbf{x}(t))+\tilde{M}(\mathbf{x}(t),\mathbf{x}(t),\mathbf{x}(t))+\sigma_1 d\mathbf{W}_1(t)+\sigma_2(\mathbf{x}(t))d\mathbf{W}_2(t). \tag{16}
$$

The qualitative new terms are the deterministic cubic operator $\tilde{M}$ and the state-dependent noise $\sigma_2(\mathbf{x})$. In general the deterministic cubic operator acts as effective damping while it also allows the system to be linearly unstable (Majda et al., 2009).

2.2. Nonlinear Deterministic Dynamics

The nonlinear deterministic dynamics for the climate variables x_1 and x_2 of the conceptual climate model (1) is given by

$$\frac{dx_1}{dt} = -x_2(L_{12} + a_1x_1 + a_2x_2)dt + d_1x_1dt + F_1dt \quad (17a)$$

$$\frac{dx_2}{dt} = x_1(L_{21} + a_1x_1 + a_2x_2)dt + d_2x_2dt + F_2dt. \quad (17b)$$

Here we set $y_1 = y_2 = 0$ in order to explore the bifurcation behaviour of the climate modes.

By varying the forcing $\mathbf{F}$ the system (15) undergoes several bifurcations as shown by Majda et al. (2005). By decreasing F_1 starting from -0.1 the system undergoes first a saddle-node bifurcation with two stable states, at the second bifurcation point a homoclinic orbit appears before it undergoes a supercritical Hopf bifurcation. For more details about the bifurcation structure of the nonlinear deterministic dynamics (17) see Majda et al. (2005) (See their Fig. 3.2 for the bifurcation diagram).

2.3. Model Integration Details

A 5000 member ensemble is created by integrating the model for 10^5 time units starting from 5000 different initial conditions which were chosen randomly and using different stochastic noise realizations. To integrate the model we are using a fourth order Runge-Kutta scheme for the deterministic part and an Euler forward scheme for the stochastic part. We use a time step of 10^{-4} time units and save output every $\frac{1}{8}$ time unit.

Furthermore, we use the three time scale separation values $\varepsilon = 0.1, 0.5$ and 1.0. These three cases correspond to time scale separation ($\varepsilon = 0.1$), moderate time scale separation ($\varepsilon = 0.5$) and no time scale separation ($\varepsilon = 1.0$). The reduced order model is only valid in case of time scale separation but in most natural system we have only moderate or no time scale separation. For instance, the atmospheric circulation has ε values between 0.6 and 1.0 (e.g. Franzke et al. (2005); Franzke and Majda (2006)). Thus, we also have to test how well the method works in these more realistic cases.

A series of studies has shown that the stochastic mode reduction performs reasonably well also for moderate or no time scale separation (Majda et al., 2002, 2005, 2008; Franzke et al., 2005; Franzke and Majda, 2006; Franzke, 2012).

3. Prediction of non-Stationary Dynamics

In this section we will evaluate how well the reduced stochastic models reproduce the full dynamics when driven by a time-dependent forcing $\mathbf{F}(t)$. First we use $F_1(t) = -0.2 + 0.4 * \sin(t/5000)$ which is a periodic forcing on a very slow time scale. The forcing has been chosen in such a way that it passes through all bifurcation points. Typical realizations can be seen in Fig. 1 for three different time scale separations. As can be seen the conceptual model exhibits different dynamical regimes for different forcing values. Furthermore, the reduced model captures this behavior very well for all three time scale separation values ε. This is further confirmed by the autocorrelation function and the PDF. The reduced order model captures the decay of the autocorrelation function (Fig. 2) and of the PDFs (Fig. 3) very well for all time scale separations. For $\varepsilon = 0.1$ the full and reduced dynamics are almost indistinguishable. The shape of the highly non-Gaussian PDFs are very well captured for both the marginal and joint PDFs by the reduced model (Fig. 4) for all three values of ε. Also in the case with no time scale separation $\varepsilon = 1.0$ the PDF is very well captured which is a very promising result since in realistic systems one rarely has time scale separation.

Now we evaluate how well the reduced model performs if the time periodic forcing drives one of the fast modes. We use $F_3(t) = -0.2 + 0.4 * \sin(t/5000)$ which is a slow periodic driving of the fast mode y_1. Also in this case the reduced stochastic model reproduces the statistics of the full dynamics very well. Again the autocorrelation function is extremely well captured for $\varepsilon = 0.1$ and still well for $\varepsilon = 0.5$ and $\varepsilon = 1.0$ (Fig. 5). To put this into context, the stochastic mode reduction strategy is strictly valid only in the limit $\varepsilon \to 0$ but as our empirical results show it still performs well in cases with no time scale separation at all. This is a promising result suggesting that our proposed approach will also work for observed data which likely has only moderate time scale separation.

4. Prediction of Tipping Points

In this section we discuss the role of time scale separation and coupling strength and how well the reduced order models predict tipping points by driving the models with a linearly increasing forcing $F_1(t) = -0.5+0.00002*t$. In figure 6 we display two example trajectories one for weak ($\theta = 0.1$) and one for strong ($\theta = 1.0$) coupling between climate and fast modes. In both cases we set $\varepsilon = 0.1$. The here relevant major difference between the two cases is the level of variability; for weak coupling the variability is much smaller and the system tips later. Furthermore, the reduced dynamics capture the full dynamics again very well.

Another way of looking at the non-stationary evolution of the conceptual model is to compute time evolving PDFs. Here we compute the PDF at a fixed time t over the 5000 member ensemble. This will reveal how narrow the window of tipping is and how well the reduced dynamics captures this essential part of the non-stationary behavior.

A comparison of the time evolving marginal PDFs (Figs. 7 and 8) shows that for weak coupling there is a rather sharply defined tipping time because the PDFs are very narrow and do not overlap during the state transition. This is also very well captured by the reduced dynamics. This is different in the case of strong coupling (Fig. 8) where the PDF is much broader and there is a rather smooth transition between the two states indicating that the tipping time is not well defined and the system tends to tip early or jumps a couple of times between both equilibrium states before it settles down on the surviving equilibrium state. However, in the case of time scale separation ($\varepsilon = 0.1$) the PDF is much sharper, though not as sharp as for the weak coupling case. Also the time window when the system tips is much narrower than for moderate time scale separation. This shows that the typical tipping point prediction methods are likely to only robustly work in the case of time scale separation and weak coupling. In other situations, which are likely more realistic, the system might not undergo a clear critical transition and flickers between the two equilibrium states.

The reduced dynamics reproduces the full dynamics very well in the case of time scale separation ($\varepsilon = 0.1$) and reasonably well in the other two cases for both weak and strong coupling. This shows the reduced order models can play a useful role in predicting tipping points.

The traditional tipping point indicators are sensitive to the way the time series is detrended and the length of the window length. Here we can use the ensemble to test whether ensemble averaging detects the critical slowing down signal. For this purpose we compute the lag-1 correlation coefficient $< x(t)x(t-1) >$ as used in the AR(1) tipping indicators and the variance $< x(t)^2 >$ at time t, where $<>$ denotes an ensemble average. This approach has the advantage that no detrending is necessary, since any trend between two consecutive time points will be negligibly small, and we also do not have to define a window length for the averaging.

Fig. 9 shows one time series realization for both climate modes in the case of weak coupling which we consider to be the truth here together with the ensemble lag-1 correlation and variance tipping point indicators averaged over 1000 ensemble members. The variance indicator increases in magnitude when approaching the tipping time. The amount of time scale separation determines when the variance reaches its maximum. For $\varepsilon = 0.1$ the variance reaches its maximum at about the time of tipping while for $\varepsilon = 1.0$ it reaches its maximum before the time of tipping and actually already decreases before the tipping. On the other hand, the lag-1 indicator increases in value only for $\varepsilon = 0.1$. In this case it also reaches its maximum before the tipping time and starts the decrease by the time of tipping. For the other two cases the lag-1 indicator is rather flat or only minimaly increasing. Thus, our model results suggest that the amount of time scale separation and the coupling strength between resolved and unresolved modes determine whether the critical transition is due to critical slowing down or flickering.

In the case of strong coupling both indicators increase before the time of tipping in the case of $\varepsilon = 0.1$ whereas in the other two cases, with only moderate or no time scale separation, the system jumps a few times between both equilibrium states (Fig. 10). But in these two cases both indicators seem to peak at about the time that the start of the transition to the other equilibrium point becomes visible in the PDF (Fig. 8). This suggests that the ensemble approach can still be useful in predicting the onset of the switch to another equilibrium point even though it is not a clear tipping point but flickering. This suggests that the ensemble approach might be useful as an early warning system even though there will be no clear or unique time of tipping.

Now we discuss how well the traditional tipping point indicators perform. In Fig. 11 we display the results of the full dynamics simulations from using 4 typical tipping point indicators: AR(1), variance, skewness and linear decay rate derived from the quasi-stationary density (Gardiner, 1985; Livina et al., 2012; Sieber and Thompson, 2012). To compute these indicators we use a sliding window of length 1000 and then linearly detrend the time series in each window. Here we average over the window length and not the ensemble. While the AR(1), variance and skewness are standard quantities the quasi-stationary density involves the Fokker-Planck equation. This indicator assumes that the deterministic dynamics of the detrended time series evolves in a potential well $U(x)$ (Gardiner, 1985; Sieber and Thompson, 2012). The linear decay rate κ can then be computed via

$$\frac{1}{2}\partial_x p(x) = -\kappa x p(x) + c \tag{18}$$

where $p(x)$ denotes the empirical density and c a constant. We approximate the derivative of the density with finite differences. We apply these 4 indicators to 100 ensemble time series for the weak coupling and $\varepsilon = 0.1$ case which can be considered to be the best case scenario for tipping point predictions. During the displayed time range in Fig. 11 both stable equilibria exist (compare with Fig. 6).

The results display a wide variety of tipping indicator behavior. It is clearly visible that, even though the PDFs (Fig. 8c) show a very narrow tipping time range, the indicators do not seem to robustly signal the imminent tipping point in our model experiments. For some realizations the indicators do not predict a tipping at all while when they predict a tipping the timing varies widely (Fig. 11). This is the case for all 4 tipping point indicators. At least for this model experiment our proposed ensemble model prediction system seems to perform more robustly and reliably.

5. Summary

Using a conceptual model mimicing aspects of complex climate models we elucidated the tipping point behaviour and how it depends on time scale separation and the coupling strength between resolved and unresolved modes. We find that for model experiments the theory of critical slowing down applies best to the case of large time scale separation and weak coupling between resolved and unresolved modes. In this situation there is a clear and distinct tipping event. For moderate or small time scale separation and strong coupling the model flickers between the two equilibrium states. Both critical slowing down (Scheffer et al., 2009; Sieber and Thompson, 2012; Livina et al., 2012) and flickering (Scheffer et al., 2009; Lenton, 2011) have been proposed as indicators of imminent tippings and here we have shown which properties of the underlying dynamics are responsible for these two distinct behaviours preceeding a critical transition.

Furthermore, we have shown that reduced order models are able to reproduce the tipping point behaviour of more complex models. Our model results suggest that predicting the time of tipping works best for systems with time scale separation and weak coupling between the resolved and the unresolved part of the system. As can be seen in Fig. 10 for strong coupling and lack of time scale separation the system flickers between the two equilibrium states. The reduced order models well reproduce this flickering.

A potential advantage of the proposed dynamical tipping prediction approach is that the reduced order models can be run in forecast mode with extrapolation of the forcing. These ensemble predictions will provide a probabilistic forecast of the tipping time which can then be used in integrated assessment and decision making models. This is not possible with the diagnostic tipping indicators which cannot provide any estimate of the tipping time other than that the system might approach the tipping point. Furthermore, the extrapolation can be done also with an ensemble of possible and plausible forcings or control parameters. This ensemble can then be used to make probabilistic forecasts about whether a tipping is imminent or not.

The stochastic mode reduction approach described here requires the knowledge of the dynamical equations of the system of interest. For the climate system the normal forms of stochastic climate models have been derived by Majda et al. (2009). In order to estimate the necessary parameter values of the stochastic differential equation from data one can use Bayesian inference methods which also takes proper account of all uncertainties (Peavoy et al., 2013). However, these approaches need to be extended to work in a non-stationary setting. Conceptually this is straight forward by treating the forcing or the control parameter as an additional equation. This forcing or the control parameter are not necessarily directly observationable. In this case it can be treated as a latent variable in Bayesian inference (Peavoy et al., 2013). This dynamical model fitting approach also offers the possibility of further insight into the underlying mechanisms of observed critical transitions. For instance, the structure of the additional equation describing the forcing could either be an increasing or decreasing function or a noise driven stationary process. In the latter case all critical transitions would likely be noise induced.

In many areas of science the evolution equations are not known. In this situation one can use non-parametric approaches to estimate the evolution equations just from observed data (Crommelin and Vanden-Eijnden, 2006; Carpenter and Brock, 2011) or fit a potential well type equation with additive noise (Livina et al., 2010, 2011; Sieber and Thompson, 2012). These approaches are more general and can be applied to many observational data sets.

Our results suggest that any early warning system of tipping points should include an ensemble approach using dynamical models. This would allow for a probabilistic prediction of imminent tipping points and would provide an estimated range of tipping times which might be useful to decide on the best avoidance or mitigation strategies by taking all uncertainties into account.

Acknowledgments I thank Drs. V. Livina and P. Ditlevsen for their comments on an earlier draft of this manuscript which helped to improve it. This study is part of the British Antarctic Survey Polar Science for Planet Earth Programme. It was funded by The Natural Environment Research Council and through NERC grant NE/G015317/1.

References

References

R. Biggs, S. R. Carpenter and W. A. Brock, Turning back from the brink: Detecting an impending regime shift in time to avert it. Proc. Nat. Acad. Sci. USA, 106 (2009), 826-831.

C. Boettinger and A. Hastings, Early warning signals and the prosecutor's fallacy. Proc. Roy. Soc. B, (2012a), doi:10.1098/rspb.2012.2085.

C. Boettinger and A. Hastings, Quantifying limits to detection of early warning for critical transitions. J. R. Soc. Interface, (2012b), doi:10.1098/rspb.2012.2085.

S. R. Carpenter and W. A. Brock, Early warnings of unknown nonlinear shifts: a nonparametric approach. Ecology, 92 (2011), 2196-2201.

A. A. Cimatoribus, S. S. Drijfhout, V. Livina and G. van der Schrier, Dansgaard-Oeschger events: bifurcation points in the climate system. Clim. Past., 9 (2013), 323-333.

D. Crommelin and E. Vanden-Eijnden, Reconstruction of diffusions using spectral data from timeseries. Comm. Math. Sci., 4 (2006), 651-668.

V. Dakos, M. Scheffer, E. H. van Nes, V. Brovkin, V. Petoukhov and H. Held, Slowing down as an early warning signal for abrupt climate change. Proc. Nat. Acad. Sci. USA, 105, 14308-14312 (2008)

P. D. Ditlevsen and S. J. Johnsen, Tipping points: Early warning and wishful thinking. Geophys. Res. Lett., 37, L19703 (2010)

I. Eisenmann and J. S. Wettlaufer, Nonlinear threshold behavior during the loss of Arctic sea ice. Proc. Nat. Acad. Sci. USA, 106 (2008), 28-32.

C. Franzke, A. J. Majda and E. Vanden-Eijnden, 2005: Low-Order Stochastic Mode Reduction for a Realistic Barotropic Model Climate. J. Atmos. Sci., 62, 1722-1745.

C. Franzke and A. J. Majda, 2006: Low-Order Stochastic Mode Reduction for a Prototype Atmospheric GCM. J. Atmos. Sci., 63, 457-479.

C. Franzke, A. J. Majda and G. Branstator, 2007: The origin of nonlinear signatures of Planetary Wave Dynamics: Mean Phase Space Tendencies and Contributions from Non-Gaussianity. J. Atmos. Sci., 64, 3987-4003. doi: 10.1175/2006JAS2221.1

C. Franzke, Predictability of extreme events in a nonlinear stochastic-dynamical model. Phys. Rev. E, 85 (2012) doi: 10.1103/PhysRevE.85.031134

C. W. Gardiner, Handbook of stochastic methods, 1985. Springer-Verlag, 442pp.

V. Guttal and C. Jayaprakash, Changing skewness: an early warning signal of regime shifts in ecosystems. Ecology Lett., 11 (2009), 450-460.

H. Held and T. Kleinen, Detection of climate system bifurcations by degenerate fingerprinting. Geophys. Res. Lett., 31, L23207 (2004) doi: 10.1029/2004GL020972

C. Kuehn, A mathematical framework for critical transitions: Bifurcations, fast-slow systems and stochastic dynamics. Physica D, 240 (2011) 1020-1035.

C. Kuehn, A mathematical framework for critical transitions: Normal forms, variance and applications. J. Nonlin. Sci., 23 (2013) 457-510.

T. M. Lenton, H. Held, E. Kriegler, J. W. Hall, W. Lucht, S. Rahmstorff and H. J. Schellnhuber, Tipping elements in the Earth's climate system. Proc. Nat. Acad. Sci. USA, 105 (2008) 1786-1793

T. M. Lenton, Early warning of climate tipping points. Nature Climate Change, 1 (2011) 201-209

V. N. Livina and T. M. Lenton, A modified method for detecting incipient bifurcations in a dynamical system. Geophys. Res. Lett., L03712 (2007) doi: 10.1029/2006GL028672

V. N. Livina, F. Kwasniok and T. M. Lenton, Potential analysis reveals changing number of climate states during the last 60kyr. Clim. Past, 6, 77-82. (2010).

V. N. Livina, F. Kwasniok, G. Lohmann, J. W. Kantelhardt and T. M. Lenton, Changing climate states and stability: from pliocene to present, Clim. Dyn., 37, 2437-2453. (2011).

V. N. Livina, P. D. Ditlevsen and T. M. Lenton, An independent test of methods of detecting system states and bifurcations in time-series data. Physica A, 391, 485-496. (2012).

V. N. Livina, G. Lohmann, M. Muddelsee and T. M. Lenton, Forecasting the underlying potential governing the time series of a dynamical system. Physica A, in press. doi: 10.1016/j.physa.2013.04.036

A. J. Majda, I. Timofeyev and E. Vanden-Eijnden, 1999: Models for stochastic climate prediction. Proc. Nat. Acad. Sci. USA, 96, 14687-14691.

A. J. Majda, I. Timofeyev and E. Vanden-Eijnden, 2001: A mathematical framework for stochastic climate models. Commun. Pure Appl. Math., 54, 891-974.

A. J. Majda, I. Timofeyev and E. Vanden-Eijnden, 2002: A priori tests of a stochastic mode reduction strategy. Physica D, 170, 206-252.

A. J. Majda, R. Abramov and M. Grote, 2005: Information Theory and Stochastics for Multiscale Nonlinear Systems. CRM Monograph Series, American Mathematical Society.

A. J. Majda, C. Franzke and B. Khouider, 2008: An applied mathematics perspective on stochastic modelling for climate. Phil. Trans. R. Soc. A, 366, 2429-2455.

A. J. Majda, C. Franzke and D. Crommelin, 2009: Normal forms for reduced stochastic climate models. Proc. Nat. Acad. Sci. USA, 106, 3649-3653. doi: 10.1073/pnas.0900173106

P. E. McSharry, L. A. Smith and L. Tarassenko: Prediction of epileptic seizures: are nonlinear methods relevant? Proc. Nature Med. (2003), 9, 241-242.

A. H. Monahan, J. Alexander and A. J. Weaver: Stochastic models of the meridional overturning circulation: time scales and patterns of variability. Phil. Trans. Roy. Soc. A (2008), 366, 2527-2544.

D. Peavoy, C. Franzke and G. Roberts: Systematic Physics Constrained Parameter Estimation of Stochastic Differential Equations. Comp. Stat. Data Analys. (2013), in preparation.

J. Ridley, J. M. Gregory, P. Huybrechts and J. Lowe: Thresholds for irreversible decline of the Greenland ice sheet. Clim. Dyn. (2010), 35, 1049-1057. doi: 10.1007/s00382-0646-0

M. Scheffer, S. R. Carpenter, J. A. Foley, C. Folke and B. Walker, Catastrophic shifts in ecosystems. Nature, 413 (2001), 591-596.

M. Scheffer, J. Bascompte, W. A. Brock, V. Brovkin, S. R. Carpenter, V. Dakos, H. Held, E. H van Mes, M. Rietkerk and G. Sugihara, Early-warning signals for critical transitions. Nature, 461 (2009) 53-59

J. Sieber and J. M. T. Thompson, Nonlinear softening as a predictive precursor to climate tipping. Phil. Trans. Roy. Soc. A, 370 (2012) 1166-1184

D. Sornette and A. Johansen, Large financial crashes. Physica A, 245 (1997), 411-422.

P. Sura, M. Newman, C. Penland and P. Sardeshmuhk, Multiplicative noise and non-Gaussianity: A paradigm for atmospheric regimes? J. Atmos. Sci., 62 (2005), 1391-1409.

A. J. Veraart, E. J. Faassen, V. Dakos, E. H. van Nes, M. Lürling and M. Scheffer, Recovery rates reflect distance to a tipping point in a living system. Nature, 481 (2012), 357-359.

P. Wadhams, Arctic ice cover, ice thickness and tipping points. J. Human Environment, 41 (2012), 23-33.

C. Wissel, A universal law of the characteristic return time near thresholds. Oecologica, 65 (1984), 101-107.

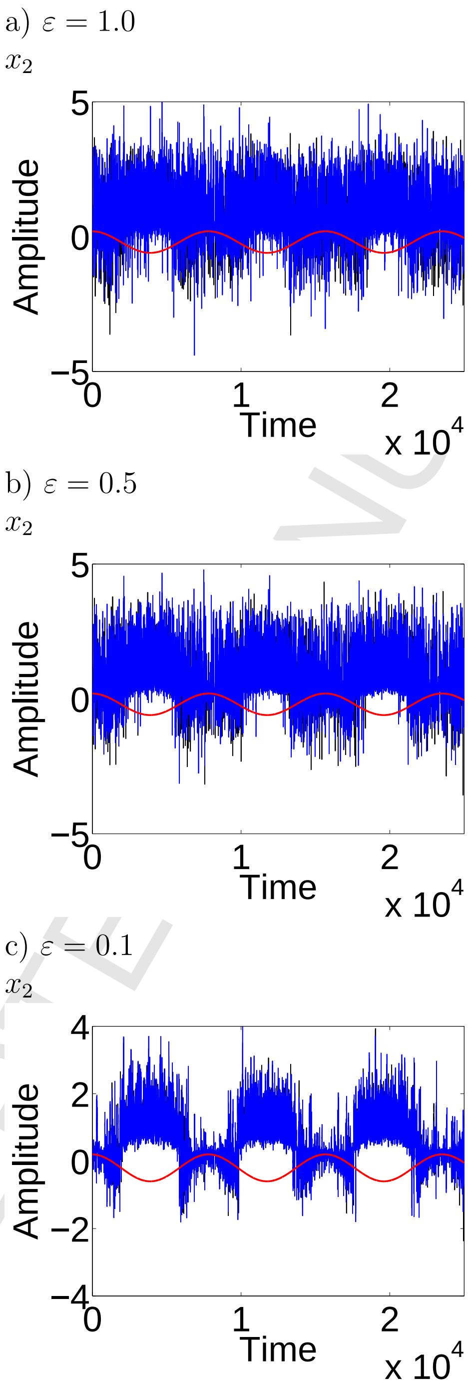

Figure 1: Section of one time series realisation for model simulations with forcing of resolved mode x_1: Black line: full dynamics; blue line: reduced dynamics; red line: Forcing.

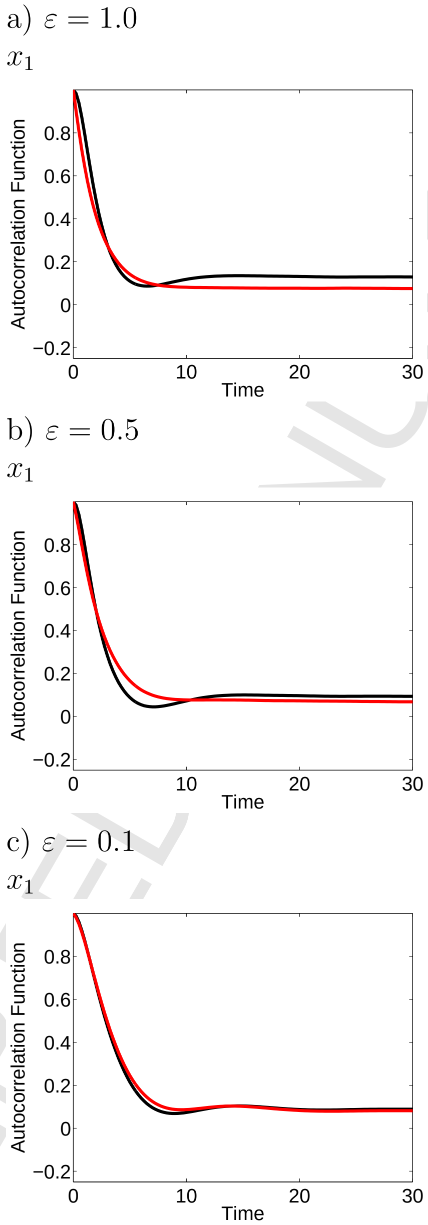

Figure 2: Autocorrelation function of model simulations with forcing of resolved mode x_1: Black line: full dynamics; Red line: reduced dynamics.

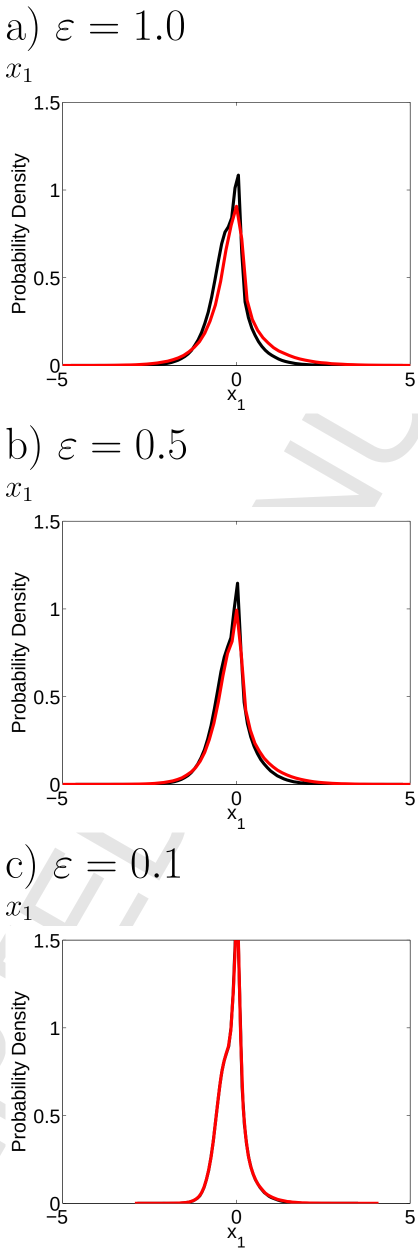

Figure 3: Marginal PDFs of model simulations with forcing of resolved mode x_1. Black line: full dynamics; Red line: reduced dynamics.

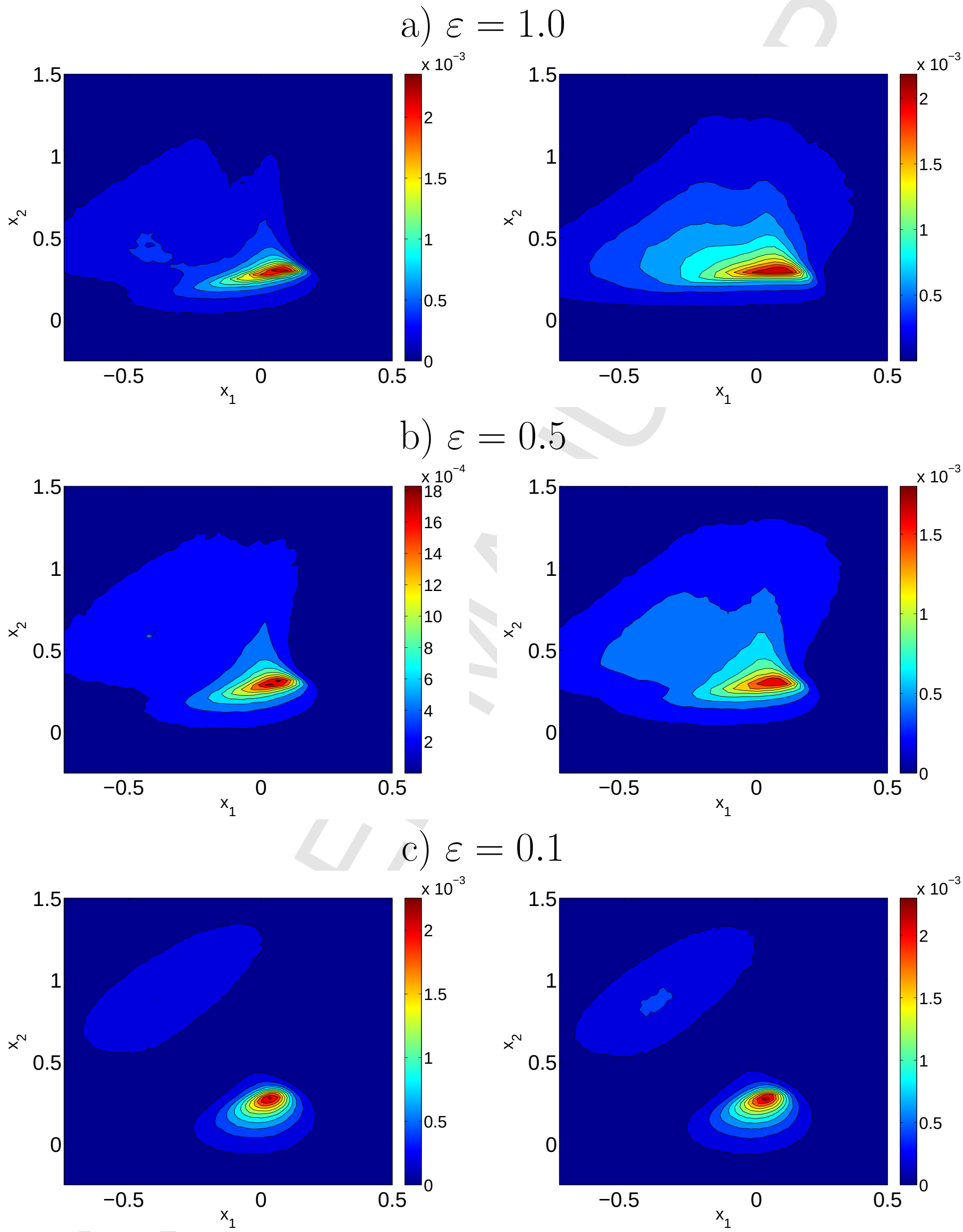

Figure 4: Joint PDFs of model simulations with forcing of resolved mode x_1: a) $\varepsilon = 1.0$, b) $\varepsilon = 0.5$, c) $\varepsilon = 0.1$. Left column: full dynamics, Right column: reduced dynamics.

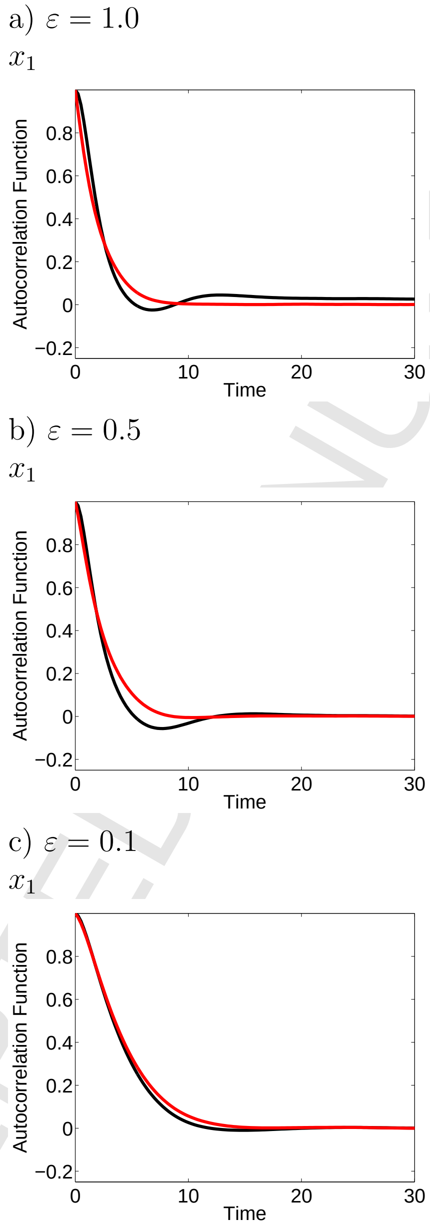

Figure 5: Autocorrelation function of model simulations with forcing of unresolved mode x_3:; Black line: full dynamics; Red line: reduced dynamics.

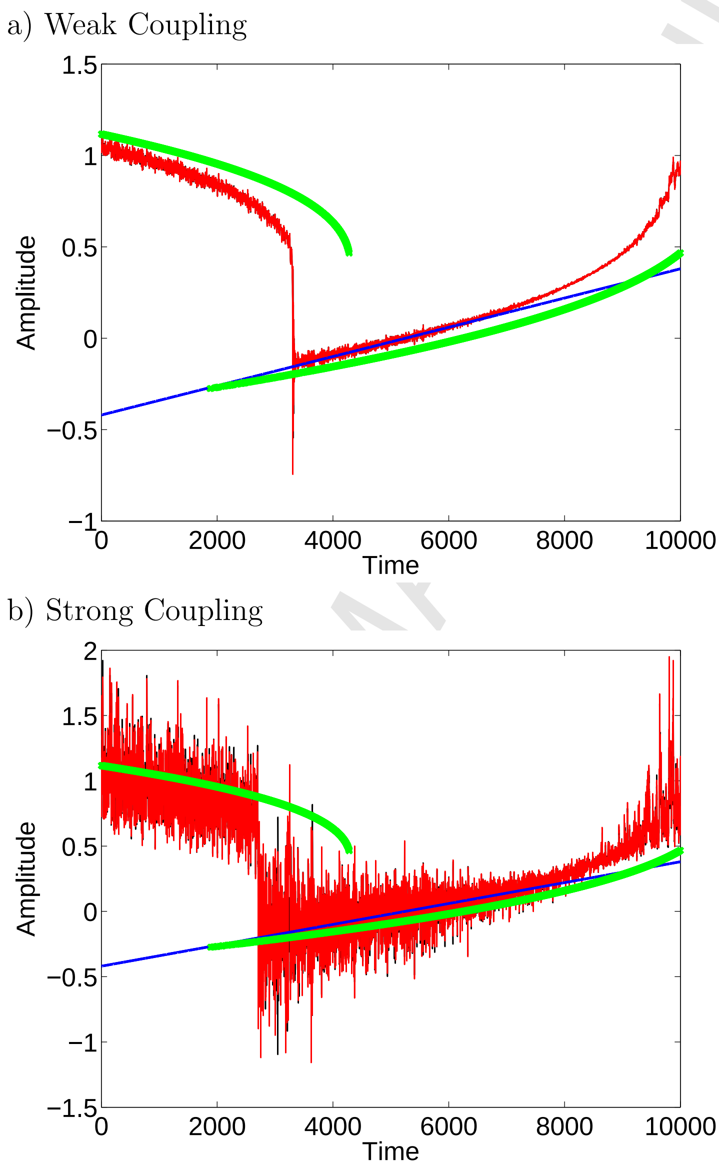

Figure 6: Time series of full dynamics (black line), reduced dynamics (red line) and forcing $F_1(t)$ (blue line) for $\varepsilon = 0.1$. The green lines indicate the equilibrium solutions of the nonlinear deterministic system (17).

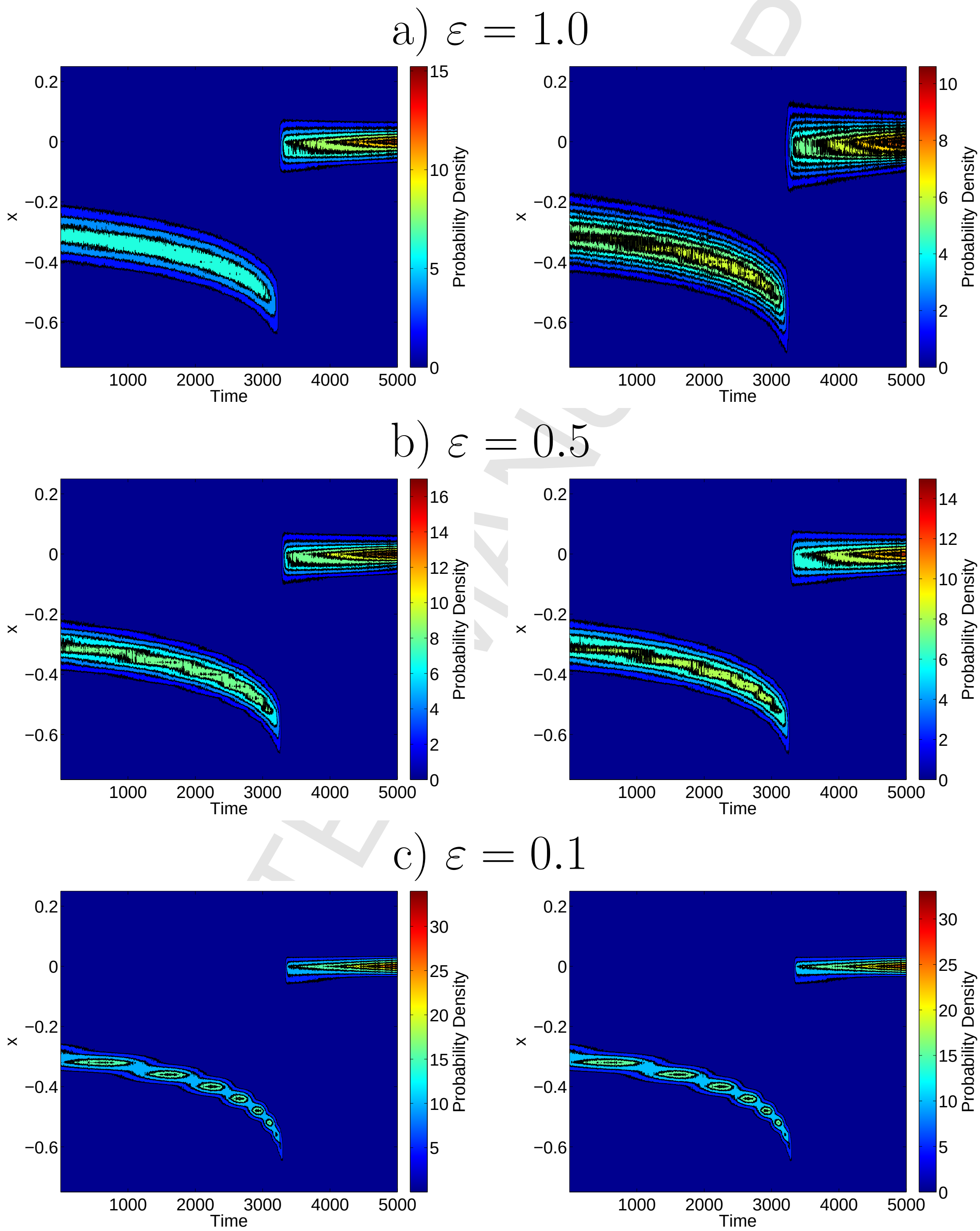

Figure 7: Marginal PDFs of x_2 from 5000 member ensemble at time t for weak coupling of resolved and unresolved modes. Left column: full dynamics; Right column: reduced dynamics.

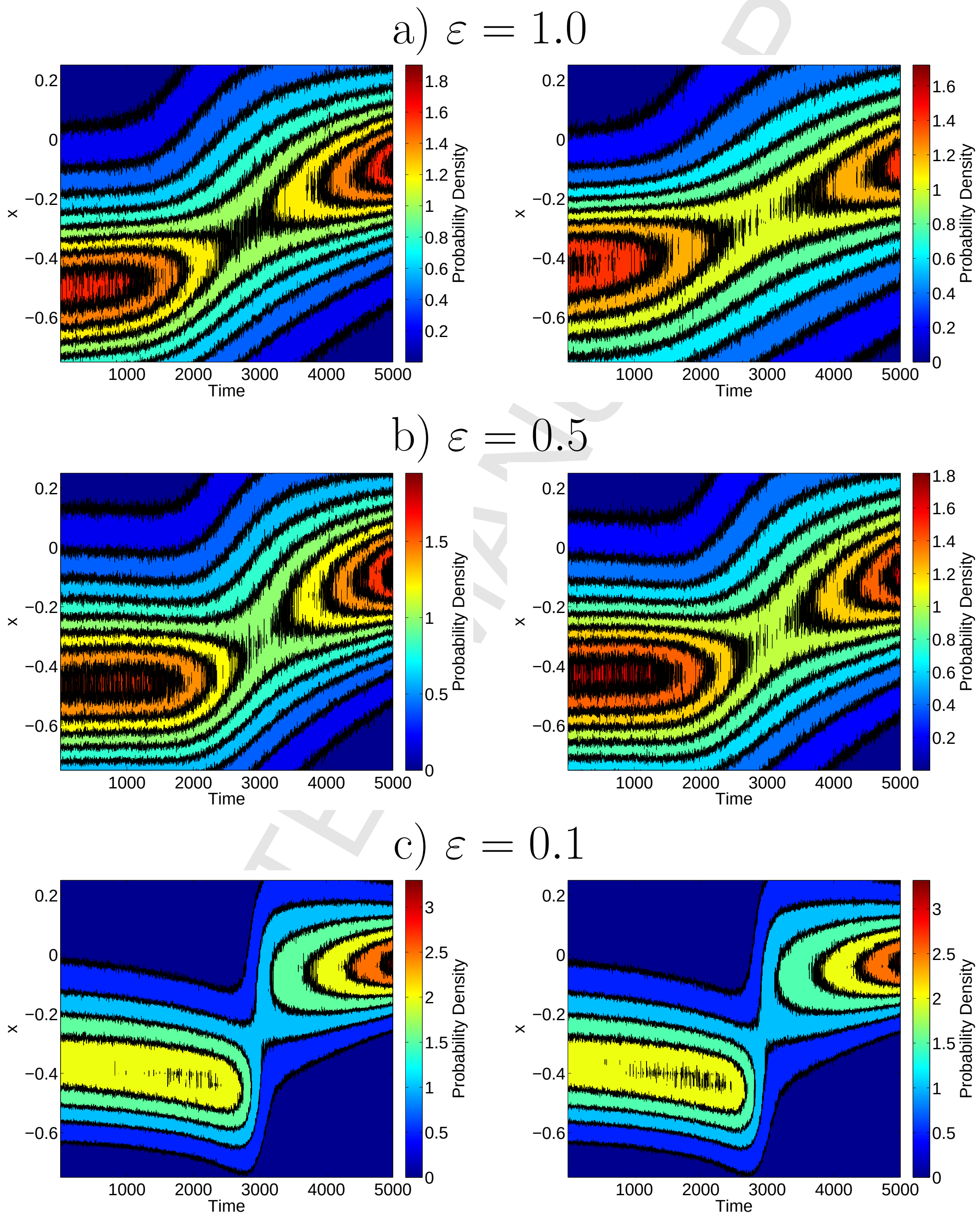

Figure 8: Marginal PDFs of x_2 from 5000 member ensemble at time t for strong coupling of resolved and unresolved modes. Left column: full dynamics; Right column: reduced dynamics.

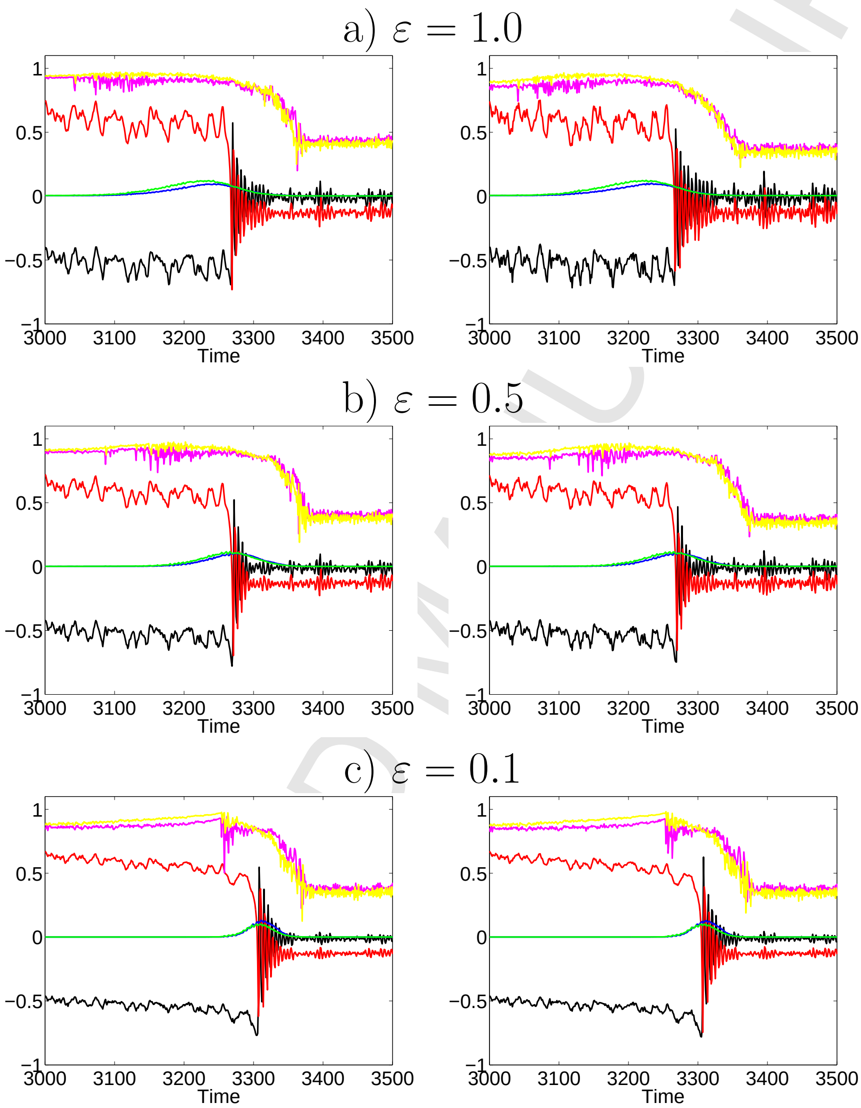

Figure 9: Ensemble indicator for weak coupling simulations. Left column: full dynamics; Right column: reduced dynamics. Black line: x_1, Red line: x_2, Blue line: ensemble variance of x_1, Green line: ensemble variance of x_1, Magenta line: ensemble AR(1) indicator of x_1, Yellow line: ensemble AR(1) indicator of x_2.

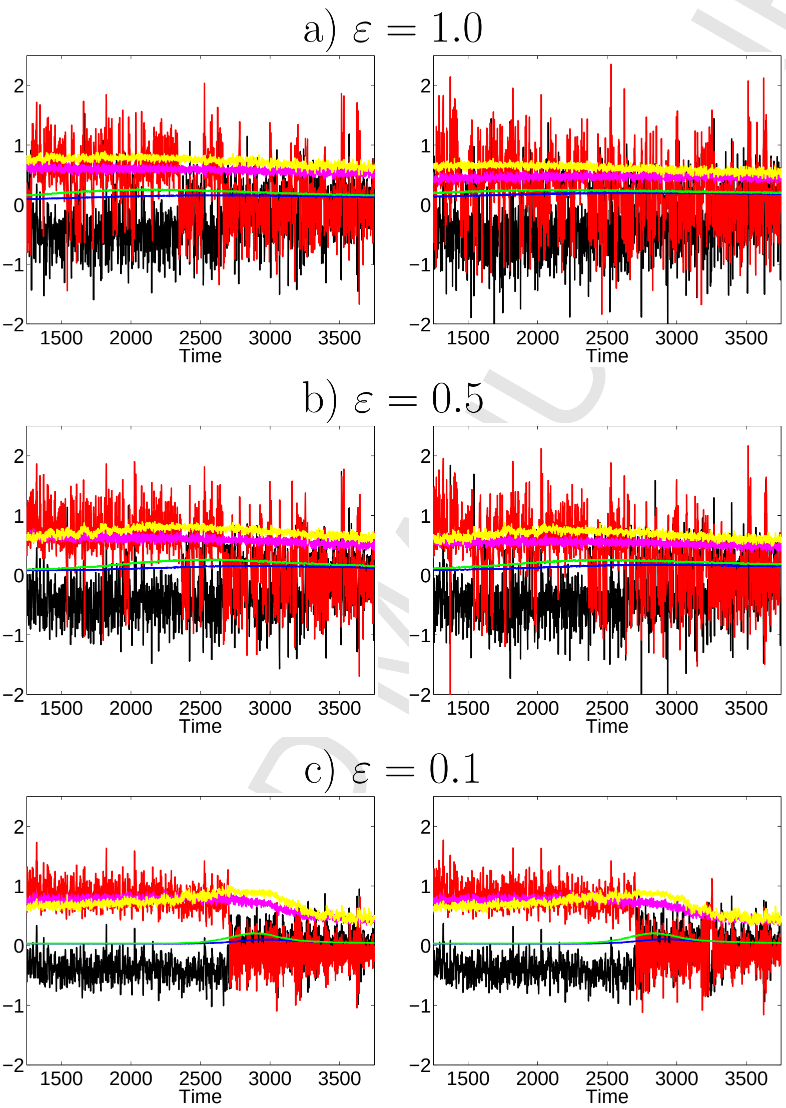

Figure 10: Ensemble indicator for strong coupling simulations. Left column: full dynamics; Right column: reduced dynamics. Black line: x_1, Red line: x_2, Blue line: ensemble variance of x_1, Green line: ensemble variance of x_2, Magenta line: ensemble AR(1) indicator of x_1, Yellow line: ensemble AR(1) indicator of x_2.

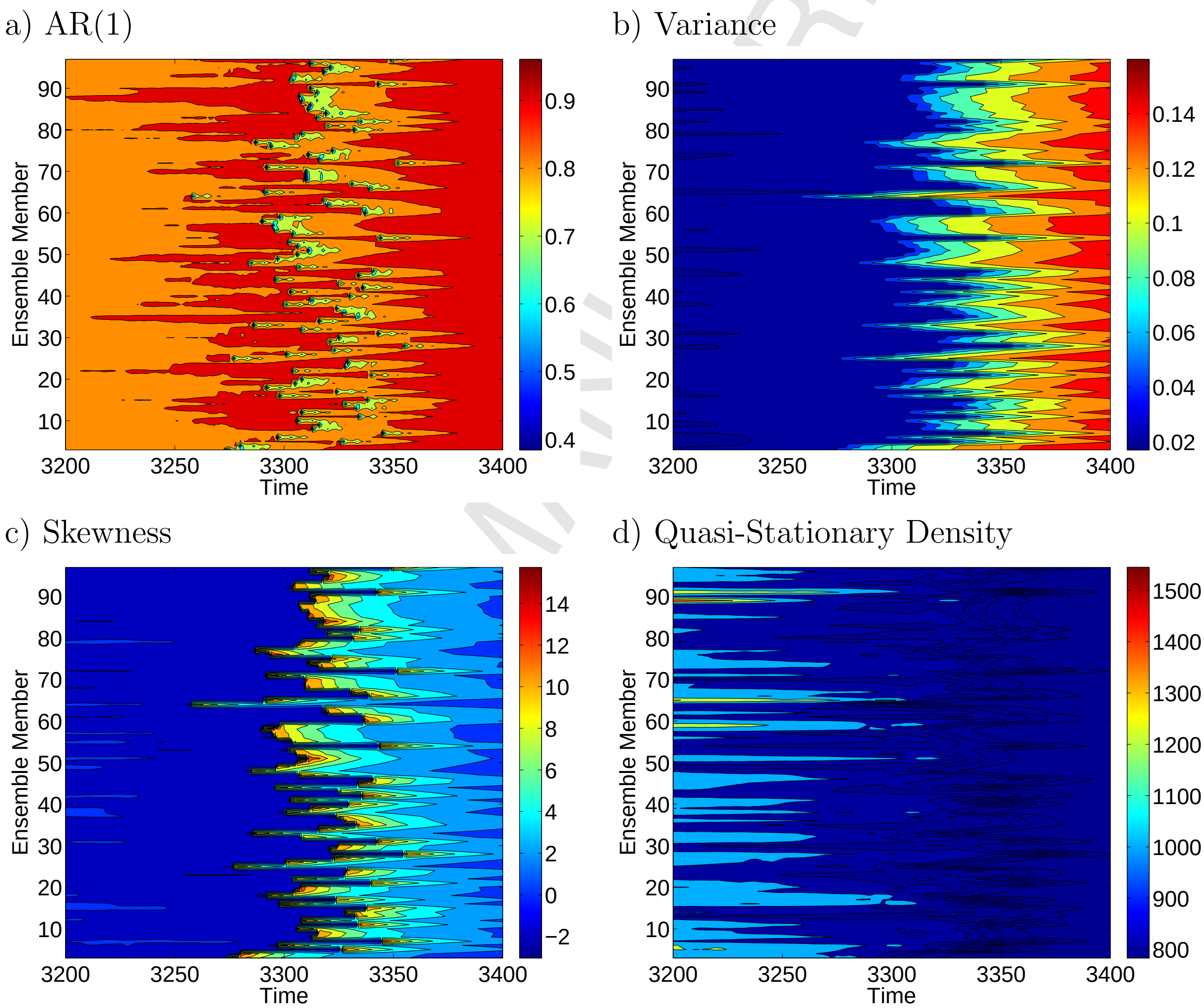

Figure 11: Tipping indicators applied to linearly detrended data from the full dynamics simulations over moving windows of length 1000 time units.